J of Nuclear Medicine Technology, first published online January 14, 2016 as doi:10.2967/jnmt.115.165258

Determining the minimal required radioactivity of ^{18}F-FDG for reliable semi-quantification in PET-CT imaging: a phantom study

Ming-Kai Chen[1], David H. Menard III[2], David W. Cheng[3], Diagnostic Radiology, Yale University School of Medicine[1], Yale-New Haven Hospital[2], and Sidra Medical and Research Center[3]

Corresponding

David W. Cheng, M.D., Ph.D.

Division Chief of Molecular Imaging and Nuclear Medicine

Associate Professor of Clinical Radiology

Weill Cornell Medical College

Sidra Medical and Research Center

PO Box 26999, Doha, Qatar

Phone: 974-4012-5936

dcheng@sidra.org

ABSTRACT:

Purpose: To investigate the minimal required radioactivity and corresponding imaging time for reliable semi-quantification in PET-CT imaging to perform useful and comparable imaging studies in pursuit of as low as reasonably achievable (ALARA) in dose reduction.

Materials and Methods: We performed ^{18}F-FDG PET-CT study using a Jaszczak ECT phantom containing spheres of diameters (3.4, 2.1, 1.5, 1.2, 1.0 cm) filled with a fixed concentration of 165 kBq/ml and background of 23.3 kBq/ml at multiple time points over 20 hours of radioactive decay. The images were acquired for 10 minutes in a single bed position at each of 10 half-lives of decay using 3D list mode in a hybrid GE Discovery 690 PET-CT scanner. The images were reconstructed in 1, 2, 3, 4, 5, and 10 minutes per bed using ordered-subset expectation maximum (OSEM) algorithm with 24 subsets and 2 iterations with a gaussian 2-mm filter using an AW workstation (GE Healthcare) equipped with version 4.5 software. The maximum and average standardized uptake values (SUV) of each sphere were measured.

Results: The minimal required activity concentration for precise SUVmax quantification in spheres (±10%) was determined to be 1.8 kBq/ml for 10 minutes, 3.7 kBq/ml for 3-5 minutes, 7.9 kBq/ml for 2 minutes, and 17.4 kBq/ml for 1 minute of acquisition per bed position. The minimal required value for the product of activity concentration and acquisition time per bed position was determined to be 10-15 kBq/ml*min for reproducible SUV measurement within the spheres without overestimation. Using the total radioactivity and count rate from the entire phantom, the minimal required values for the product with time per bed position was determined to be 17 MBq*min and 100 kcps*min, respectively.

Conclusion: Our phantom study determined a threshold for minimal radioactivity and acquisition time for precise semi-quantification in FDG PET imaging that can serve as a guide in pursuit of achieving ALARA.

Key Words: PET, phantom, dosimetry, dose reduction, acquisition time, standard uptake value, SUV, ALARA

INTRODUCTION

There is a growing trend to minimize ionizing radiation exposure, in particular, from diagnostic medical imaging involving x-ray and internal radiation from administration of radionuclides. Recent evidence from a retrospective large cohort study of over 178,600 UK residents with radiation exposure from CT scans in childhood assessed a relative risk of 3.18 for leukemia with a cumulative dose of >30 mGy, obtainable from as few as 5-10 head CT scans in patients under 15 years of age, and a relative risk of 2.82 for brain cancer with a cumulative dose of 50-74 mGy, obtainable from as few as 2-3 head CT scans, as compared to a cumulative dose of <5 mGy *(1)*. In a study of 680,000 Australians exposed to CT scans in childhood and adolescence, Mathews et al reported an incidence rate ratio of 1.24 for all cancers with an observed dose-response relation of 0.16 per additional CT scan using an estimated average effective radiation dose of 4.5 mSv per scan *(2)*.

^{18}F-FDG PET-CT scans have been widely used for oncology and cardiac imaging, with radiation exposures derived from injected dose of radiotracer and transmission x-ray from CT imaging for anatomical co-registration and attenuation correction. Previous studies suggested the effective dose from PET-CT to be in the range of 10-30 mSv depending on the activity of ^{18}F-FDG injected (0.02 mSv/MBq, according to ICRP publication 106) and CT protocols (1-20 mSv) *(3, 4, 5, 6, 7)*. In light of recent evidence for potential cancer risks related to radiation exposure from medical imaging studies *(1, 2, 7)*, we have determined a dose reduction from 555 MBq (15 mCi) to 370 MBq (10 mCi) did not affect our semi-quantitation of maximal standard

uptake value (SUVmax) and image quality *(8)*. However, we suspected that further reduction in dose can be accommodated without affecting SUV quantitation or image quality using our standard 3 minute per bed PET data acquisition. Murray et al. *(9)* demonstrated biases introduced by low statistics using time-of-flight (TOF) technology. Although our scanner is TOF capable, we feel TOF-SUVs may have limited usefulness, given there are many more non-TOF capable PET/CT scanners our patients may access for follow-up studies. Furthermore, Murray et al. did not explore the threshold in counting statistics or report a practical parameter (e.g. minimum count rate for each bed position) which can guide adjustments in PET acquisition time to maintain precision in SUVs. The aim of this study is to investigate the effects of count rate and total accumulated counts on the precision and accuracy of quantification, in order to determine the parameters necessary to obtain useful PET-CT studies that can be directly compared to previous studies, a very important (but often overlooked) consideration in maintaining continuity of care for clinicians.

METHOD AND MATERIALS:

A hybrid GE PET-CT Discovery 690 (D-690) scanner is equipped with a lutetium-yttrium-orthosilicate (LYSO) detector and a 64-slice CT. GE D-690 scanner has a design detection block of 54 (9 x 6) of individual LYSO crystals (dimensions of 4.2 x 6.3 x 25 mm^3), coupled to a single squared photomultiplier tube with 4 anodes *(10)*. The D690 consists of 24 rings of detectors (total 13824 LYSO crystals) for an axial field of view (FOV) of 157 mm. The transaxial FOV is 70 cm. The D690 uses a low energy threshold of 425 keV and a coincidence time window of 4.9 ns *(10)*. The D690 operates in 3D mode only. The CT of D690 is

LightSpeed VCT with 912 channels x 64 rows, which allows full 360 degree rotation scans with variable time ranging from 0.35 to 2 sec and slice thickness of 64 x 0.625 mm, 32 x 1.25 mm, 16 x 2.5 mm, 8 x 5 mm and 4 x 10 mm *(10)*.

We acquired PET-CT images using a standard Jaszczak ECT phantom Model ECT/STD/P (Data Spectrum Corporation , Hillsborough, NC), modified with hollow spheres of various diameters (3.4, 2.1, 1.5, 1.2, 1.0, and 0.5 cm) filled with a fixed concentration of 165 kBq/ml and a background radioactivity of 23.3 kBq/ml of ^{18}F-FDG, for a target/background ratio of 7, at multiple time points over 20 hours of radioactive decay (Figure 1). Images were acquired for 10 minutes in a single bed position in list mode approximately every 2 hours of decay and reconstructed into 1, 2, 3, 4, 5, and 10 mins acquisitions using ordered-subset expectation maximum (OSEM) algorithm with 24 subsets and 2 iterations with a gaussian 2-mm filter using an AW workstation (GE Healthcare) equipped with version 4.5 software using registered CT (120 kVp and 50-90 mA) for attenuation correction.

The radioactivity of the spheres with both maximal and average standardized uptake value (SUV) were measured by applying volume of interests (VOI) of spheres with a threshold 41% of maximal value in serial PET images using a GE Advanced Workstation. We also checked co-registered CT imaging and adjusted the size of VOI accordingly to make sure all VOIs were placed correctly. The SUV computation was derived from the radioactivity concentration (kBq/ml) divided by total administered radioactivity within the phantom (kBq) and normalzied to total weight of the phantom (g). Because of the inclusion of phantom weight, the SUV measurement was higher than the target to backround ratio of 7. The coefficients of recovery were calculated from radioactivity in PET divided by known activity from dose

calibrator with decay correction back to the beginning time point. The variability of the SUV measurements in each sphere at various time points was calculated against the value of the first 10 min acquisition in each sphere, as our reference standard. A deviation of SUV (±10%) in comparison with reference standard can be considered acceptable in accordance to the test-retest variability of 20% for FDG PET studies *(11)*. The data were analyzed and plotted using Microsoft Excel 2010.

RESULTS:

The coefficients of recovery for SUV maximum calculated from our first acquisition (t=0) were 0.97, 0.94, 0.79, 0.71, 0.45, 0.17 for spheres with diameters of 3.4, 2.1, 1.5, 1.2, 1.0, 0.5 cm, respectively. Of note, the activity for 0.5 cm sphere in PET was not visually distinct from background and required the help of the CT image due to severe partial volume effect.

Figure 2A shows dramatic overestimation of SUVmax at very low radioactivity, up to 20.1 in the largest sphere of 3.4 cm as compared to the stable range of SUVmax 9-10. The overestimation of SUVmax could not be evaluated in smaller spheres due to severe partial volume effect. The SUVmax for the same radioactivity concentration is much less in smaller spheres as compared to the largest sphere, which is secondary to partial volume effect. Similarly but to a lesser extent, figure 2B demonstrates overestimation of SUVave in lower activity concentration up to 13.4 compared to reproducible range of 7-8. The overestimation of SUVave is also not significant in smaller spheres. Overestimation is again seen in SUVmax and SUVave in the background at lower radioactivity concentrations, with the range in SUVave being less in

smaller spheres as compared to the largest sphere at the same radioactivity concentration, which may be secondary to partial volume effects (data not shown). Of note, the values of SUVmax 9-10 were calculated based on the total weight of the phantom (including FDG solution and phatom itself) and were higher than the presumed target to background ratio of 7. If we excluded the weight of phantom, the SUVmax values should be close to 7. In fact the ratios of SUVmax for the largest sphere to backround are approximately 7.

The minimal radioactivity concentration within the spheres for reproducible SUVmax quantification was determined to be 1.8 kBq/ml for 10 minute, 3.7 kBq/ml for 3-5 minute, 7.9 kBq/ml for 2 minute, and 17.4 kBq/ml for 1 minute acquisitions based on the acceptable deviation of SUV (±10%) in all the spheres in comparison with reference standards (10 min acquisition at the beginning). The minimal activity for satisfactory visual assessment were 0.9 kBq/ml for 5 and 10 minute, 1.8 kBq/ml for 3 and 4 minute, 3.7 kBq/ml for 2 minute, and 7.9 kBq/ml for 1 minute acquisitions. The minimal count rates required from the entire phantom (or one field of view) were 10 kcps for 10 minute, 21 kcps for 3-5 minute, 44 kcps for 2 minute, and 98 kcps for 1 minute acquisitions. Figures 3A and 3B demonstrate the effect for the largest 3.4 cm diameter sphere.

When considering the product of radioactivity concentration and acquisition time per bed, the minimal required value was determined to be 10-15 kBq/ml*min for reproducible SUV measurements (±10%) (constrained to the smallest delineated sphere of 1 cm diameter, with a lower value for larger spheres) without overestimation (Figures 4B and 4C). Using the count rate from the entire phantom, the minimal required value of the count rate and acquisition time product was 100 kcps*min (data not shown).

We noticed both the SUVmax and SUVave were overestimated at very low radioactivity concentration at short acquisition times, with a greater extent in larger spheres (up to 300% in the 3.4 cm sphere at 1 minute acquisition). This is likely attributed to significant buildup of noise, with a large portion from the intrinsic contaminant radioactivity of Lutetium-176 embedded within the crystal. The average count rate without the phantom or external radioactivity was 1.1 kcps, attributed to the room environment and the intrinsic properties of the scanner.

DISCUSSION:

This study searched for the minimal required radioactivity concentration for reliable quantification in various sizes of spheres as surrogates for FDG-avid lesions of various sizes. Furthermore, the image sets acquired over the ten half-lives of decay simulated lesions of the same size with different FDG-avidity (proportional to count rates), in order to better understand compensatory effects from increased total counts to improve counting statistics. We determined a minimal required count rate for the entire phantom with various length of acquisition times by calculating a product of radioactivity concentration (or count rate) and duration of acquisition time. Using these data, we could estimate a minimal required injection dose to a human patient that would provide the required count rate in the body and in lesions of various sizes appropriate for an imaging protocol of 3 min/bed acquisition. It may be possible to further reduce the injected dose, and hence, the radiation exposure and absorbed dose, to patients by extending the acquisition time to 4-5 minutes or longer. Conversely, if a patient cannot tolerate a 3 minutes per bed acquisition, we can use this model to estimate a higher dose administration appropriate for a corresponding shorter acquisition time.

The version 1.0 of European Association of Nuclear Medicine (EANM) procedure guidelines for tumor PET imaging recommended FDG dosing of 5 MBq/kg body weight (±10%) for 2D scans and 2.5 MBq/kg for 3D scans based on a duration of 5 minutes per bed position and bed overlap of less than 25% *(12)*. Alternate dosing for different durations per bed position can be calculated using their equations for varying body weight (MBq/kg), 2D vs 3D scans and bed overlap (25% vs 50%) equipped with LSO, LYSO, or GSO crystal *(13)*. They reported that the FDG activity in MBq could be as low as 6.9 x weight / acquisition (min/bed) or 2.3 MBq/kg for 3 min/bed acquisition using a bed overlap of 50%. According to our phantom data, the minimal required total activity at the time of imaging for reproducible quantification is 3.6 MBq in a 9 kg phantom or 0.4 MBq/kg for 3 min/bed acquisition. Taking into account of approximately 20-25% urine excretion *(6, 13, 14)* and 1 hour decay during distribution uptake after injection, the weight based injected dose may translate to approximately 0.8 MBq/kg using 3 minutes per bed acquisition in the GE D690 PET-CT scanner. Since our estimates were under ideal parameters, more conservative adjustments may be used for heavier patients.

Previous studies for optimal injected activity and acquisition have been focused on the parameter of noise equivalent count rates (NEC) and systematic performance *(15, 16, 17, 18, 19)*. However, clinicians may utilize the reproducibility of SUV measurements as a more sensitive guide to image quality in assessing direct comparability between initial evaluation and treatment response PET images. Any reduction in the injected dose from published recommended protocols or guidelines will translate into a lower cumulative dose for each patient, which will be especially important for those requiring 3-4 PET-CT studies a year with good long-term survival.

Overestimation of SUV maximum and SUV average in spheres at very low radioactivity concentrations have been observed. They may be explained through low counting statistics and intrinsic (background) radioactivity of the LYSO crystal. Overestimation of SUVmax has been reported from noisier imaging using only a small portion of total counts in a respiratory gated study *(20)*. However, overestimation of SUV average may not be explained by noise buildup alone. The LYSO crystal, similar to the LSO crystal, is intrinsically radioactive due to the presence of ^{176}Lu (2.6%) in nature. The ^{176}Lu decays by β^- (mean energy of 420 keV) followed by prompt emission of γ-rays at 307 keV, 202 keV and 88 keV. The β^--particle is absorbed within the crystal of origin while the γ-rays are detected at a different crystal. Hence, this intrinsic radioactivity can produce up to 1 million counts per second as detected by the entire scanner, with a total random coincidence rate of 1600 cps in a 350-650 keV acceptance window, and falsely contributes a true coincidence rate of approximately 600 cps in a LSO scanner *(21, 22)*. The intrinsic rate can be reduced from 940 cps in a 250-750 keV energy window to less than 2 cps in a 400-750 keV window as demonstrated in a LSO-based small animal PET scanner *(23)*. The D690 PET scanner has set the lower threshold at 425 keV, and the reported intrinsic rate is significantly reduced to about 1 cps *(10)*, which can be considered negligible in clinical settings but not at very low count rates, such as in lesions with low FDG-avidity. Other explanations may include suboptimal scanner sensitivity calibration (at these low count rates), inaccurate dead-time correction (at these low count rates), or suboptimal reconstruction algorithm. Investigations using scanners by other vendors at very low counts can further support our results and conclusions.

In a recent clinical publication *(8)*, we observed the stabilization of the SUVs through counting statistics with longer acquisition times. Although our clinical protocol limited us to a maximum of 3 minutes per bed position, the count rates from the lesions were more than adequate to provide good precision in our SUVs, which allayed our concerns over whether our injected dose was sufficient to provide good contrast between pathology and physiologic biodistribution in the entire body. Schwartz et al *(24)* demonstrated the intrinsic behavior of SUVs using a large ^{68}Ge-phantom with a half-life of 271 days that enabled 30 runs of up to 30 minutes each. With the decay of our ^{18}F-FDG phantom over 10 half-lives, we were able to test the bounds within which the SUVs will remain precise. Our arduous efforts in performing this 20 hour long experiment were to maintain valid comparisons of an individual SUV at each time point to each other *(25, 26)*. Our data trend agreed with the findings of Schwartz and colleagues *(24)*, which gives us the confidence that we have accounted for the intrinsic factors in our results and able to draw valid conclusions outside of their range. Given the short half-life of ^{18}F-FDG of only 109 minutes and the unrealistic expectation of a patient laying still for longer than 3-4 minutes per bed position, the practice of ALARA in the clinical setting must be balanced by achieving sufficient count rate (and acquiring adequate total counts for good statistics) within 3-4 minutes per field of view. Otherwise, comparability between studies may come into question, especially when SUVs are used to determine changes in response to treatment. Since the sensitivity of detecting a lesion is directly dependent upon the target to background ratio, qualitative assessments, whether it is in an initial staging or restaging scan, depends solely upon the reconstructed image on the screen, and the quality of which is a direct reflection of the underlying counting statistics.

Our work can be expanded into exploring various reconstruction settings (pixel size, filters, subsets and iterations) with varying tumor-to-background ratios using an anthropomorphic phantom. Other limitations of this work include the need to validate our thresholds on clinical patients, especially since they are lower than the current EANM recommendations. We anticipate that the clinical protocol will require a higher administered dose due to physiologic urinary excretion of FDG, and hence, we tried to estimate the thresholds from count rates during the PET acquisition and be flexible with acquisition times to obtain good statistics. To our knowledge, this approach has not been explored or reported as a way to implement ALARA to patients and nuclear medicine staff while maintaining comparable SUVs. Murray et al. proposed lowering injected doses only for response to chemotherapy studies but not for baseline and end-of-treatment studies. ALARA can extend to all patients at all times, and the results, SUVs in particular, should be directly comparable in all studies.

CONCLUSION:

Our phantom study determined the importance of counting statistics in the overall quality and usefulness of a PET-CT study. Our quantitative approach will ensure direct comparability between longitudinal studies and enable us to determine a minimal required dose in achieving ALARA in order to minimize the risk for secondary cancers over a patient's lifetime.

DISCLOSURE

No conflict of interest relevant to this article was reported.

ACKNOWLEDGEMENT:

The authors would like to thank Chi Liu, Ph.D. for his suggestions during the preparation of this manuscript.

REFERENCES:

1. Pearce MS, Salotti JA, Little MP, et al. Radiation exposure from CT scans in childhood and subsequent risk of leukaemia and brain tumours: A retrospective cohort study. *Lancet*. 2012;380:499-505.

2. Mathews JD, Forsythe AV, Brady Z, et al. Cancer risk in 680,000 people exposed to computed tomography scans in childhood or adolescence: Data linkage study of 11 million australians. *BMJ*. 2013;346:f2360.

3. ICRP. Radiation dose to patients from radiopharmaceuticals. addendum 3 to ICRP publication 53. ICRP publication 106. approved by the commission in october 2007. *Ann ICRP*. 2008;38:1-197.

4. Brix G, Lechel U, Glatting G, et al. Radiation exposure of patients undergoing whole-body dual-modality 18F-FDG PET/CT examinations. *J Nucl Med*. 2005;46:608-613.

5. Gelfand MJ. Dosimetry of FDG PET/CT and other molecular imaging applications in pediatric patients. *Pediatr Radiol*. 2009;39 Suppl 1:S46-56.

6. Hays MT, Watson EE, Thomas SR, Stabin M. MIRD dose estimate report no. 19: Radiation absorbed dose estimates from (18)F-FDG. *J Nucl Med*. 2002;43:210-214.

7. Huang B, Law MW, Khong PL. Whole-body PET/CT scanning: Estimation of radiation dose and cancer risk. *Radiology*. 2009;251:166-174.

8. Cheng DW, Ersahin D, Staib LH, Della Latta D, Giorgetti A, d'Errico F. Using SUV as a guide to 18F-FDG dose reduction. *J Nucl Med*. 2014;55:1998-2002.

9. Murray I, Kalemis A, Glennon J, et al. Time-of-flight PET/CT using low-activity protocols: Potential implications for cancer therapy monitoring. *Eur J Nucl Med Mol Imaging*. 2010;37:1643-1653.

10. Bettinardi V, Presotto L, Rapisarda E, Picchio M, Gianolli L, Gilardi MC. Physical performance of the new hybrid PETCT discovery-690. *Med Phys*. 2011;38:5394-5411.

11. Frings V, van Velden FH, Velasquez LM, et al. Repeatability of metabolically active tumor volume measurements with FDG PET/CT in advanced gastrointestinal malignancies: A multicenter study. *Radiology*. 2014;273:539-548.

12. Boellaard R, O'Doherty MJ, Weber WA, et al. FDG PET and PET/CT: EANM procedure guidelines for tumour PET imaging: Version 1.0. *Eur J Nucl Med Mol Imaging*. 2010;37:181-200.

13. Dowd MT, Chen CT, Wendel MJ, Faulhaber PJ, Cooper MD. Radiation dose to the bladder wall from 2-[18F]fluoro-2-deoxy-D-glucose in adult humans. *J Nucl Med*. 1991;32:707-712.

14. Ruotsalainen U, Suhonen-Polvi H, Eronen E, et al. Estimated radiation dose to the newborn in FDG-PET studies. *J Nucl Med*. 1996;37:387-393.

15. Everaert H, Vanhove C, Lahoutte T, et al. Optimal dose of 18F-FDG required for whole-body PET using an LSO PET camera. *Eur J Nucl Med Mol Imaging*. 2003;30:1615-1619.

16. Inoue K, Kurosawa H, Tanaka T, Fukushi M, Moriyama N, Fujii H. Optimization of injection dose based on noise-equivalent count rate with use of an anthropomorphic pelvis phantom in three-dimensional 18F-FDG PET/CT. *Radiol Phys Technol*. 2012;5:115-122.

17. Lartizien C, Comtat C, Kinahan PE, Ferreira N, Bendriem B, Trebossen R. Optimization of injected dose based on noise equivalent count rates for 2- and 3-dimensional whole-body PET. *J Nucl Med*. 2002;43:1268-1278.

18. Watson CC, Casey ME, Bendriem B, et al. Optimizing injected dose in clinical PET by accurately modeling the counting-rate response functions specific to individual patient scans. *J Nucl Med*. 2005;46:1825-1834.

19. Masuda Y, Kondo C, Matsuo Y, Uetani M, Kusakabe K. Comparison of imaging protocols for 18F-FDG PET/CT in overweight patients: Optimizing scan duration versus administered dose. *J Nucl Med*. 2009;50:844-848.

20. Liu C, Alessio A, Pierce L, et al. Quiescent period respiratory gating for PET/CT. *Med Phys*. 2010;37:5037-5043.

21. Erdi YE, Nehmeh SA, Mulnix T, Humm JL, Watson CC. PET performance measurements for an LSO-based combined PET/CT scanner using the national electrical manufacturers association NU 2-2001 standard. *J Nucl Med*. 2004;45:813-821.

22. Watson CC, Casey ME, Eriksson L, Mulnix T, Adams D, Bendriem B. NEMA NU 2 performance tests for scanners with intrinsic radioactivity. *J Nucl Med*. 2004;45:822-826.

23. Goertzen AL, Stout DB, Thompson CJ. A method for measuring the energy spectrum of coincidence events in positron emission tomography. *Phys Med Biol*. 2010;55:535-549.

24. Schwartz J, Humm JL, Gonen M, et al. Repeatability of SUV measurements in serial PET. *Med Phys*. 2011;38:2629-2638.

25. Boellaard R, Krak NC, Hoekstra OS, Lammertsma AA. Effects of noise, image resolution, and ROI definition on the accuracy of standard uptake values: A simulation study. *J Nucl Med*. 2004;45:1519-1527.

26. Keyes JW,Jr. SUV: Standard uptake or silly useless value? *J Nucl Med*. 1995;36:1836-1839.

FIGURE 1

A

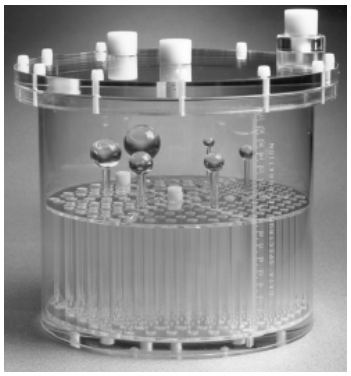

B

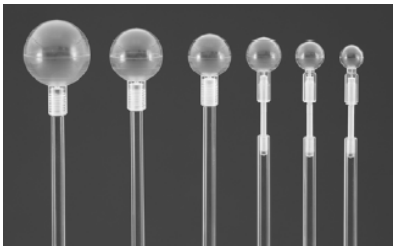

C

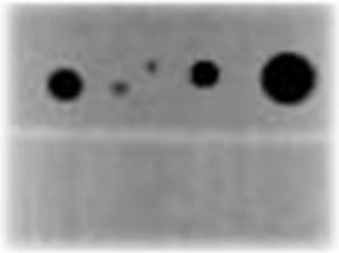

D

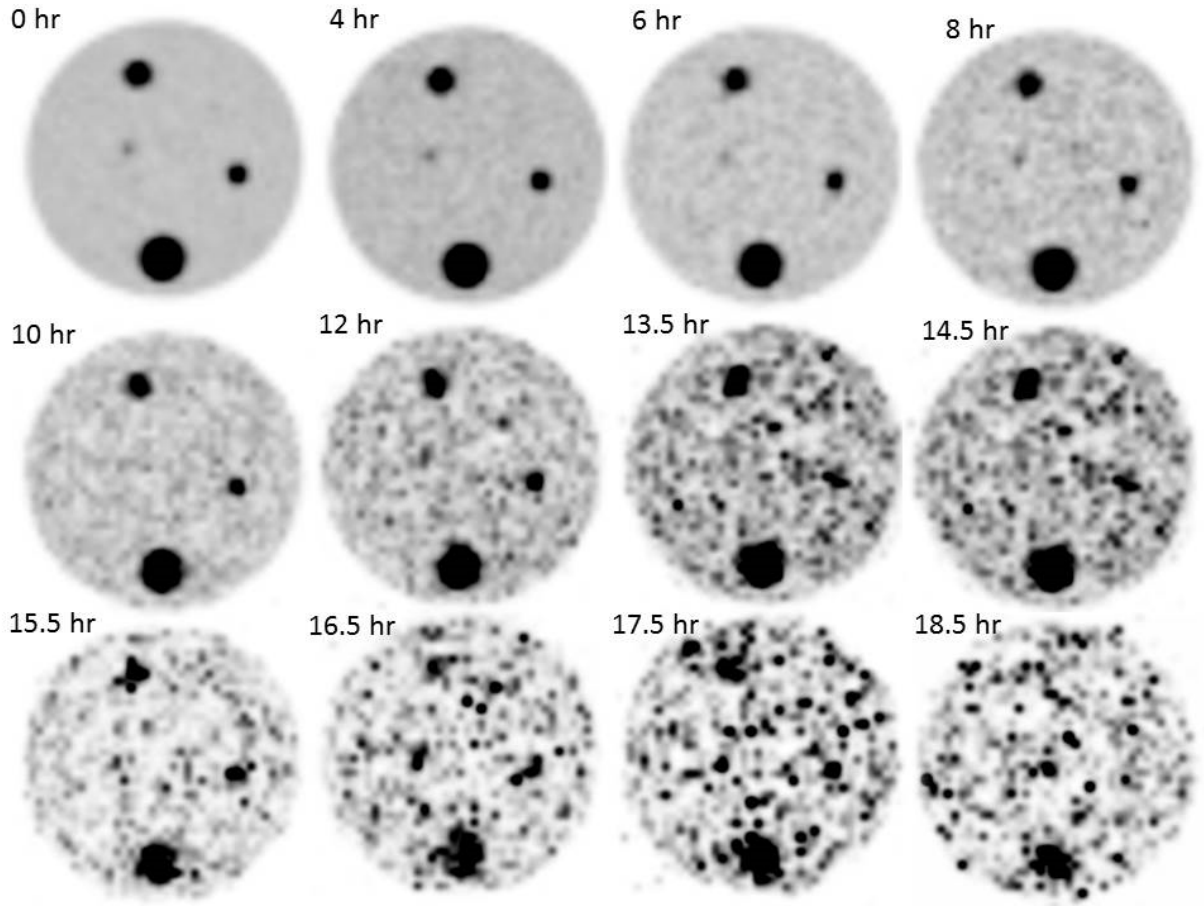

Figure 1. The standard Jaszczak ECT phantom with solid spheres (A) was replaced by various sizes of hollow spheres (diameters of 3.4, 2.1, 1.5, 1.2, 1.0, 0.5 cm) (B), filled with 165 kBq/ml FDG (C), and transaxial reconstructed images at 0, 4, 6, 8, 10, 12, 13.5, 14.5, 15.5, 16.5, 17.5, and 18.5 hours of decay (displayed in 3 min reconstruction) (D).

FIGURE 2A

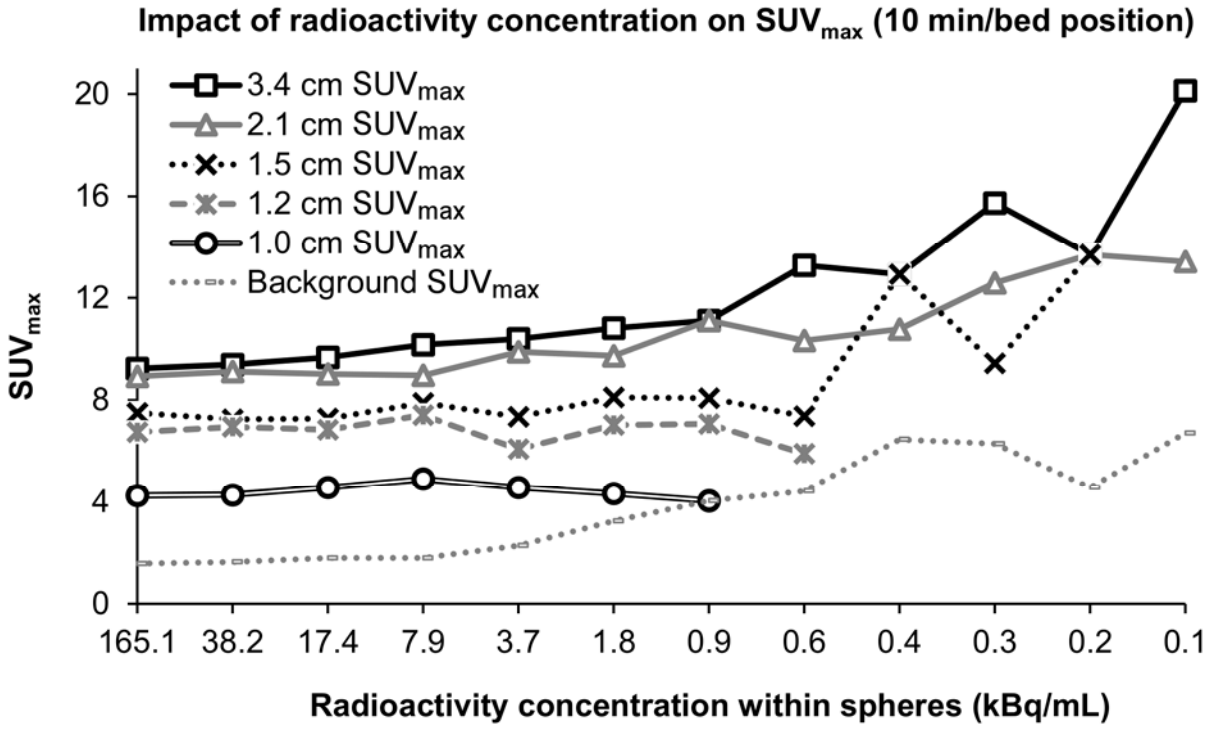

FIGURE 2B

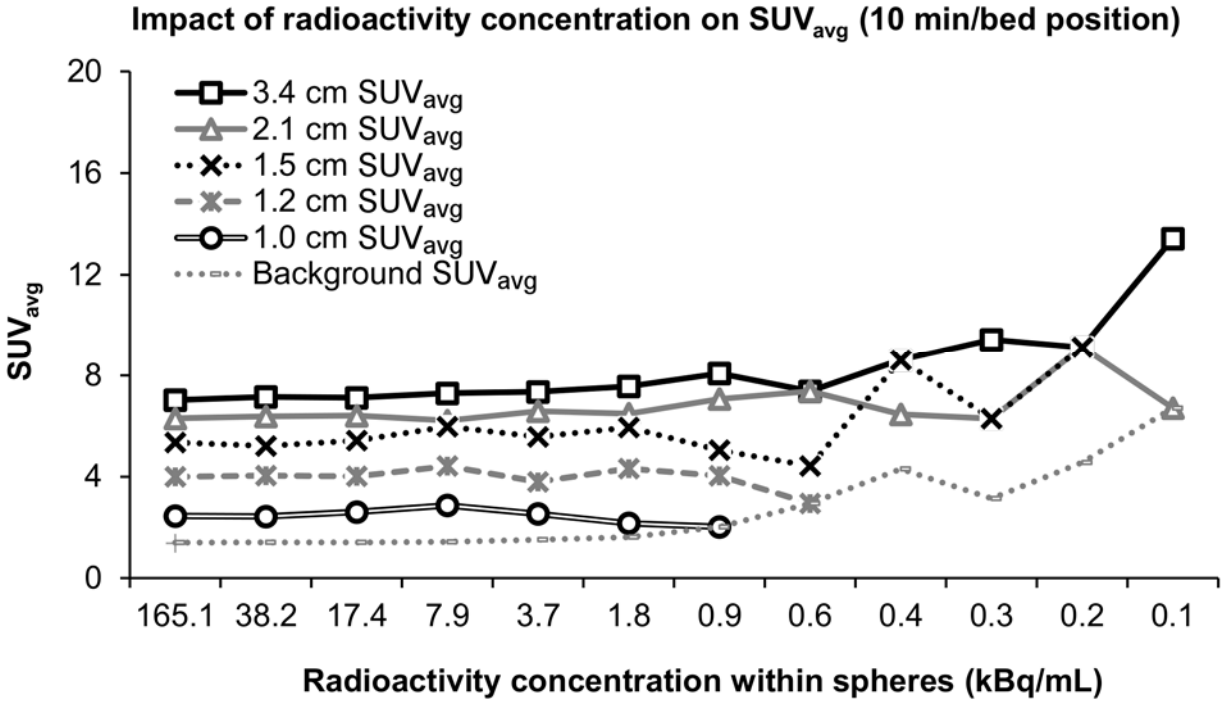

Figure 2. Impact of radioactivity concentration on maximal and average SUVs in various sizes of spheres using a 10 min acquisition.

The radioactivity concentrations on x-axis correspond to the time points of acquisition and radioactive decays at approximately 0, 4, 6, 8, 10, 12, 13.5, 14.5, 15.5, 16.5, 17.5, and 18.5 hours in figures 2A and 2B.

FIGURE 3A

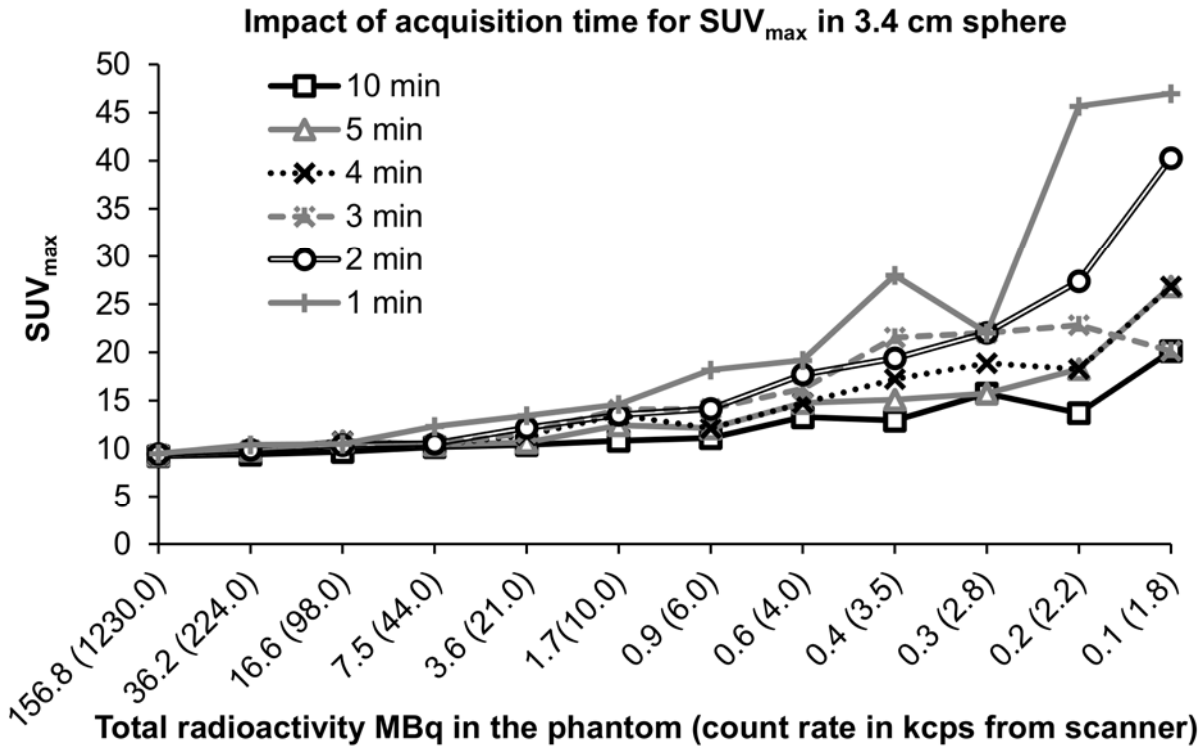
Impact of acquisition time for SUVmax in 3.4 cm sphere
SUVmax
50
45
40
35
30
25
20
15
10
5
0
10 min
5 min
4 min
3 min
2 min
1 min
156.8 (1230.0)
36.2 (224.0)
16.6 (98.0)
7.5 (44.0)
3.6 (21.0)
1.7(10.0)
0.9 (6.0)
0.6 (4.0)
0.4 (3.5)
0.3 (2.8)
0.2 (2.2)
0.1 (1.8)
Total radioactivity MBq in the phantom (count rate in kcps from scanner)

FIGURE 3B

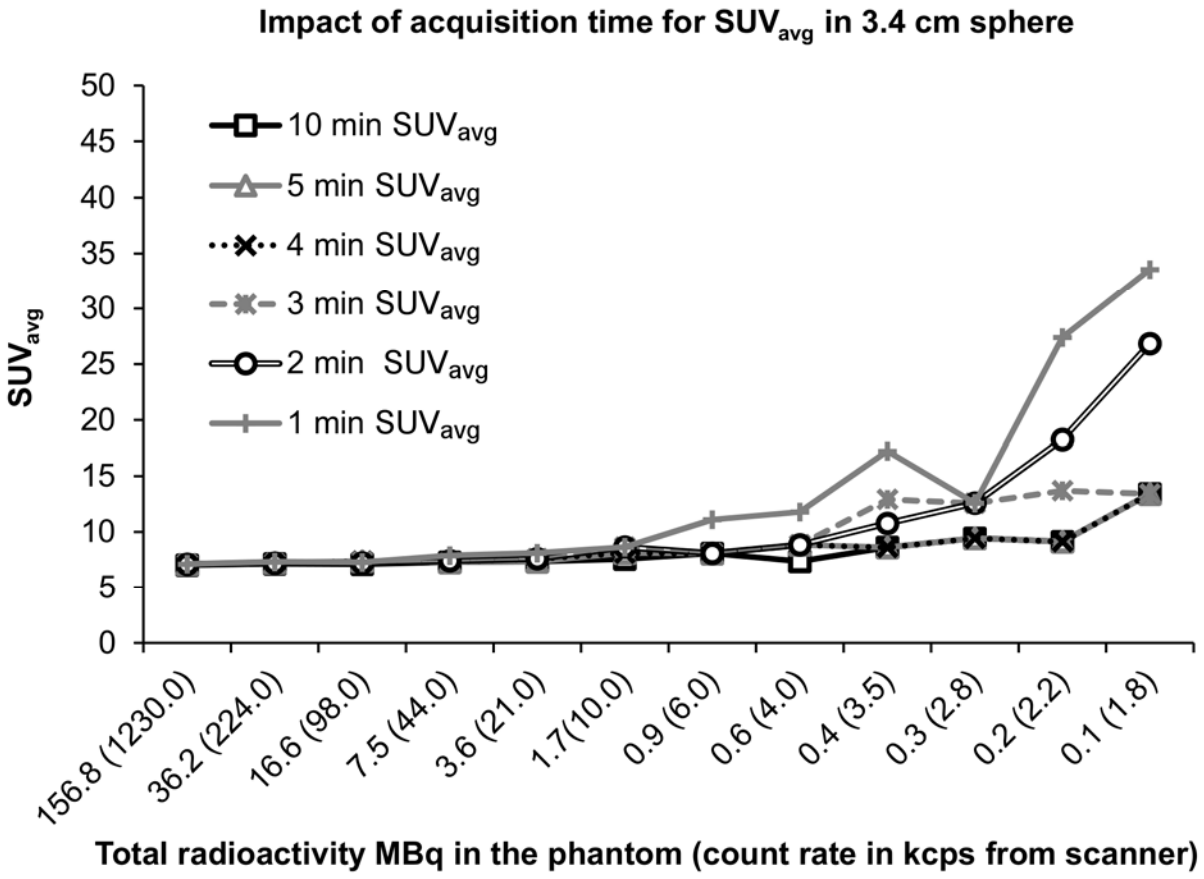

Figure 3. Impact of total radioactivity and count rates on maximal and average SUV of various acquisition times on 3.4 cm sphere.

Figure 3A shows significant overestimation of SUVmax in lower radioactivity concentration up to 47 in the shortest acquisition (1 min) as compared to reproducible range of SUVmax 9-10. Figure 3B demonstrates overestimation of SUVave in lower radioactivity concentration up to 33.6 at 1 min acquisition as compared to a reproducible range of SUVave 7-8 at longer acquisitions. The values along the x-axis represent the total radioactivity within the phantom (MBq) while the values within parentheses represent the count rates directly from the PET

scanner. Of note, the count rates from the PET scanner are total count rates with no corrections made for random counts or dead time.

FIGURE 4A

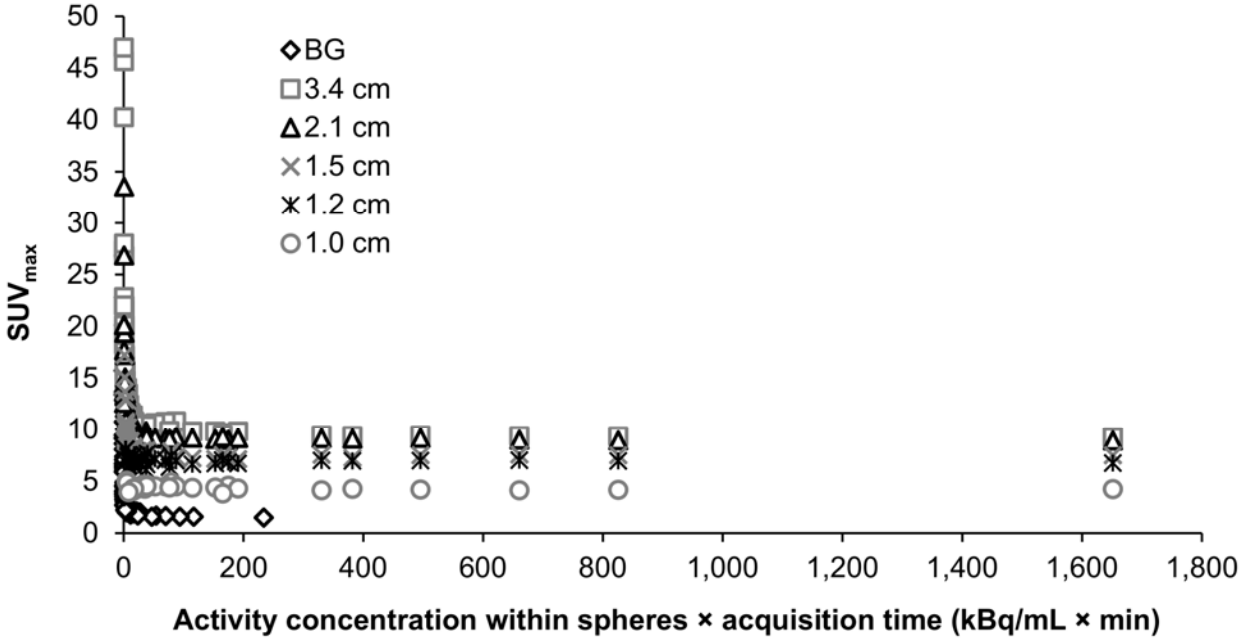

FIGURE 4B

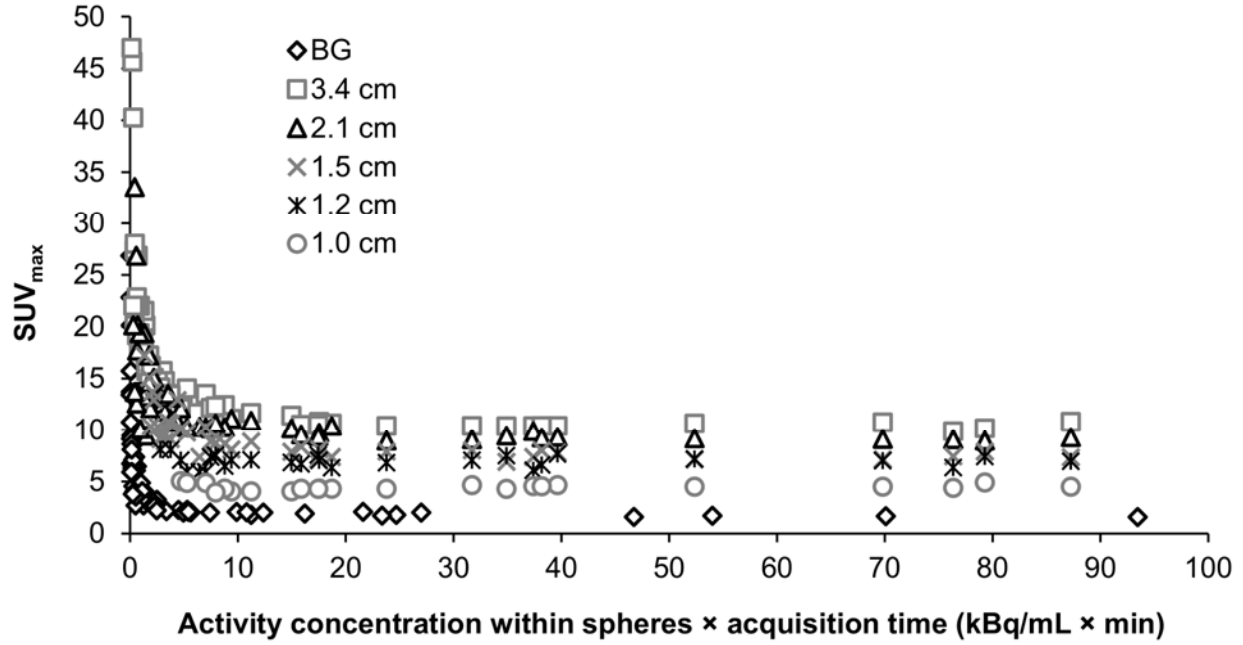

FIGURE 4C

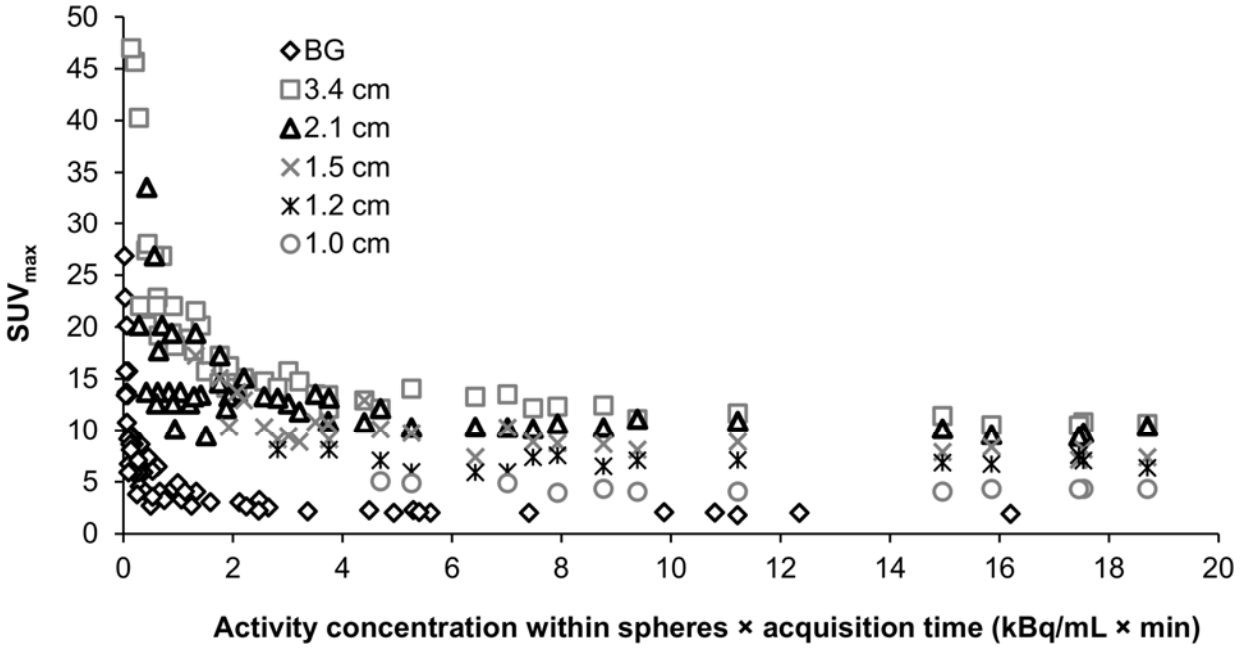

Figure 4. Using a product of radioactivity concentration and acquisition time to determine the reproducibility of SUVmax in various sizes of spheres.

Figure 4A shows SUVmax measurements as a function of the product of radioactivity concentration and acquisition time. Overestimation of SUVmax in various sizes of spheres within the very low range of product of radioactivity concentration and acquisition time is further characterized in 4B and 4C (expanded x-axis).

Table 1: Radioactivity concentration and required acquisition time for reprodicible SUV measurements

Radioactivity Concentration (kBq/ml)	Acquisition Time (min)
1.8	10
3.7	3-5
7.9	2
17.4	1